Journal of Ceramic Processing Research. Vol. 20, No. 1, pp. 113~120 (2019)

J O U R N A L O F
Ceramic Processing Research

Microstructure and mechanical properties of B_4C-TiB_2 ceramic composites hot pressed with in-situ reaction

P. Švec*, Z. Gábrišová and A. Brusilová

Institute of Technologies and Materials, Slovak University of Technology in Bratislava, Faculty of Mechanical Engineering, Pionierska 15, 831 02 Bratislava, Slovak Republic

Ceramic composite materials consisting of a boron carbide (B_4C) matrix and titanium diboride (TiB_2) secondary phase were in-situ manufactured via chemical reaction of B_4C and titanium diboride (TiO_2) during hot pressing at a temperature of 1850 °C under a pressure of 35 MPa for 60 min in a vacuum atmosphere. The TiO_2 addition has a positive effect on both densification of B_4C-TiB_2 ceramic composites and portion of TiB_2 secondary phase. When adding 10 to 50 wt.% TiO_2 to B_4C, sintered densities increased from 92.1 to 99.5% and portion of TiB_2 secondary phase increased from 3.9 to 40.2 vol.%. When increasing the TiB_2 portion to its maximal value, the fracture toughness of the composite reached the maximal value of 7.51 MPa.m$^{1/2}$. The hardness of B_4C-TiB_2 composite improved when increasing the portion of TiB_2 phase only up to the value of 29.7 vol.% when it reached the average value of 29.8 GPa.

Key words: Ceramic composite, Boron carbide, Titanium diboride, Hot pressing, In-situ reaction.

Introduction

Boron carbide (B_4C) ceramics possess excellent physical and mechanical properties with high melting points and hardness, good impact and wear resistance, excellent resistance to chemical agents as well as a high capacity for neutron absorption [1-4]. After diamond and cubic boron nitride, B_4C is the third hardest material with the hardness above 30 GPa [5-7]. It is a promising candidate for wear resistance components. Sand-blast nozzles and water jet nozzles present some example applications. Moreover, the low density of B_4C (2.52 g.cm^{-3}) and its high Young's modulus (460 GPa) recommend this material for the construction of light weight armours such as bullet-proof vests and aircraft applications. High active cross section of B_4C for neutrons absorption can be utilised in nuclear technique [7-11]. One important advantage in comparison with many ceramic materials is good electric conductivity, which enables to form products from B_4C by electrical discharge machining [12, 13]. However, this material has found limited use in industry due to its difficult sintering and its low fracture toughness value [14-18]. High temperature is required for its sintering due to a low self-diffusion coefficient [19-21]. Nearly full densification cannot be achieved by pressureless sintering but can be attained in pure B_4C by hot pressing above 2300 °C [20, 22]. Moreover, compacts sintered above 2000 °C result in entrapped residual porosity due to grain coarsening [22, 23]. Low fracture toughness (2.2 MPa.m$^{1/2}$) causes the sensitivity to brittle fracture of B_4C ceramics and constitutes a major limiting factor for application of boron carbide ceramic parts [7, 24-26].

Continuous research on boron carbide-based ceramics has shown that suitable second phase addition helps in achieving improved sintering behaviour and mechanical properties, mainly fracture toughness [27-30]. Selection of the additive and the method of consolidation are selected according to the end use of the product and the final required properties. The additive by itself or by its in-situ reaction with the main phase would form a non-volatile second phase aiding in densification and property improvement. Hence, the selection of the additive should focus on forming a suitable structure which can provide the correct properties for use [28-31].

For B_4C ceramics, effective sintering aids are carbon, aluminium, silicium, some oxides, borides, etc. [29-32]. Oxide additions as sintering aid are particularly interesting due to the chemical instability of B_4C with respect to many oxides [33]. The addition of titatinum dioxide (TiO_2) into B_4C greatly reduces the sintering temperature because of a reactive in the in-situ sintering process which involves the conversion of TiO_2 to titanium diboride (TiB_2) and therefore creation of ceramic composite material consisting of a B_4C matrix and TiB_2 secondary phase [5, 14, 34]. Reactive in-situ sintering of this system is accompanied by formation of CO and CO_2 volatile species and their portion corresponds to the

*Corresponding author:
Tel : +421-905326211
E-mail: pavol.svec@stuba.sk

weight lost during sample sintering. The TiO_2 concentration in B_4C and TiO_2 initial powder mixture has an essential effect on the density of B_4C-TiB_2 composite, the final portion of both TiB_2 secondary phase, and CO and CO_2 volatile species. With the increased ratio of TiO_2 the densification of sintered composite material will be supported, the portion of TiB_2 secondary phase will be increased and the portion of volatile species will significantly grow [12, 14].

Many researchers have shown that the TiB_2 secondary phase in the B_4C matrix supports high fracture toughness and great hardness of this ceramic composite material [15-17, 26, 32, 35, 36]. The fracture toughness of this composite increases in consequence of higher fracture toughness of the TiB_2 phase compared to B_4C phase, hence the TiB_2 phase serves as the strengthening and toughening phase in the B_4C-TiB_2 composite. Taking a closer view of the propagation of cracks in B_4C-TiB_2 composites, deflection and branching of the crack take place during its propagation into secondary phase, which relates to absorption of energy and increase of fracture toughness of the composite [7, 16, 17, 24, 37]. Although, the densification during in-situ sintering has a positive effect on hardness of B_4C-TiB_2 composite the hardness is usually lower compared to monolithic B_4C ceramics, because of the lower hardness of TiB_2 ceramics compared to B_4C [5-7, 11].

Enhanced mechanical properties of B_4C-TiB_2 composites were measured in several works. The results reported by various authors differ not only in consequence of different parameters, but also because of various preparation methods. In the work [38], B_4C-TiB_2 composites with various portions of TiB_2 and with WC contamination from the milling process enabled decreasing of the sintering temperature necessary for full densification by hot pressing to 1860 °C. The B_4C-TiB_2 composite with 25 vol.% B_4C showed the hardness of 32.2 GPa, the B_4C-TiB_2 composite with 75 vol.% TiB_2 had the fracture toughness of 5.01 $MPa.m^{1/2}$ [38]. B_4C-TiB_2 composites with 15 and 30 vol.% TiB_2 were sintered by using pulsed electric currents from B_4C, TiO_2 and carbon black mixtures in a vacuum at 2000 °C in the work [39]. The fully densified B_4C-TiB_2 composites with 30 vol.% TiB_2 had Vickers hardness of 39.3 GPa, and modest fracture toughness of 3.0 $MPa.m^{1/2}$ [39]. Positive effect of TiO_2 on the properties of B_4C-TiB_2 composites fabricated using the hot press of TiO_2, B_4C and phenolic resin was confirmed in the work [40]. The relative density of 98.2%, a hardness of 25.9 GPa, and the fracture toughness of 8.7 $MPa{\cdot}m^{1/2}$ were measured in the B_4C-TiB_2 composite with a 43 wt.% TiB_2 [40]. Authors of the work [41] manufactured TiB_2-B_4C composites with 40 vol.% B_4C by means of pulsed electric current sintering and achieved the density of 3.72 $g.cm^{-3}$, Vickers hardness of 29.45 GPa, and the fracture toughness of 4.5 $MPa.m^{1/2}$ [41]. In the work [14], the fully dense boron carbide matrix composites B_4C-TiB_2 containing from 10 to 40 vol.% TiB_2 were in-situ fabricated via a chemical reaction of B_4C, TiO_2 and graphite powders at 2050 °C under a pressure of 35 MPa. With the increase of TiB_2 content, the elastic modulus and fracture toughness of composites increased, but Vickers hardness and flexural strength decreased. The fracture toughness exhibited a maximum value of 8.2 $MPa{\cdot}m^{1/2}$ for the 40 vol.% TiB_2. The main toughening mechanisms of B_4C-TiB_2 composites were microcrack toughening and crack deflection toughening. The Vickers hardness achieved maximal value of 29.5 GPa for a composite with 10 vol.% TiB_2 [14].

The increase of both the hardness and the fracture toughness were set as goals in our paper, hot pressing was chosen as a sintering process to obtain fully dense materials with enhanced mechanical properties. TiO_2 sintering additive was used to prepare B_4C-TiB_2 ceramic composite materials with in-situ reactive sintering. The effects of TiO_2 additive concentration in the initial powder mixture consisting of B_4C and TiO_2 powders on the density and microstructure were evaluated. The effect of TiB_2 secondary phase portion in B_4C-TiB_2 ceramic composites on the hardness and the fracture toughness of these composite materials were studied.

Experimental

B_4C-TiB_2 ceramic composites were prepared by in-situ reactive hot pressing of initial powder mixtures consisting of B_4C powder with different concentration of TiO_2 sintering additive (10, 20, 30, 35, 40, 45, 50 wt.% TiO_2). Both B_4C and TiO_2 initial powders had the purity of 99% and a particle size from 2 to 3 μm and were produced by Acros Organics and Merc, respectively. Mixing using the horizontal mill in Teflon container of 450 ml volume with B_4C mill balls and an isobutyl alcohol lubricant was chosen for homogenisation of the initial powder mixtures. After milling the initial powder mixtures for 4 hours and drying on air at a temperature of 120 °C for 24 hours, they were dry milled and sieved through a 0.355 mm sieve.

Before the hot-pressing process, the initial powder mixtures were die pressed in a simple tool with a floating die of a cylindrical shape with a diameter of 8 mm and with an overall powder weight of 2 g. The powder mixtures were pressed at pressures from 120 to 150 MPa. The green bodies had cylindrical shapes with a diameter of 8 mm and height of about 25 mm. Their densities were from 1.3 to 1.8 $g.cm^{-3}$ depending on the composition of the initial powder mixture, they reached about 50% of relative density. Green bodies were consequently hot pressed in a vacuumed atmosphere at about 10 Pa. Samples were hot pressed in a graphite die with a floating matrix of cylindrical shapes with a diameter of 8 mm. The Die surface was coated by a separation layer from hexagonal BN to

prevent the joining of graphite die with the samples. All samples were hot pressed at the same temperature of 1850 °C, time of 60 min and a pressure of 35 MPa, which represents border values regarding our hot press equipment and which can eliminate grain coarsening.

The densities of hot-pressed samples were measured using the Archimedes method. The microstructures were studied on a cross section of sintered composite samples prepared by standard metallographic methods. Both the Axiovert 40MAT light microscope (LM) and JEOL JSM-IT300 scanning electron microscope (SEM) were used for the microstructure observation. The phase analysis was done using a X-ray diffraction method with Philips PW 1710 diffractometer with source of characteristic X ray of cobalt $l_{Ka1,2}$. Volume portions of identified phases were measured using image analysis with the Multiphase module of AxioVision software. The hardness and fracture toughness were measured by the indentation method using a Vickers indenter with load of 5 kP (49.03 N) and indentation time of 10 s. The fracture toughness of B_4C-TiB_2 ceramic composites were calculated using the formula $K_{IC} = 0.203Ha^{1/2}(c/a)^{-3/2}$, where H is the hardness, a is the impression radius, and c is the radial-median crack length measured on the impression.

Results and Discussion

The densification, microstructure, phase composition and the mechanical properties of the ceramic composite material B_4C-TiB_2 prepared by reactive in-situ hot pressing of powder mixtures B_4C and TiO_2 with the initial composition from 10 to 50 wt.% TiO_2 were evaluated.

Densification of B_4C-TiO_2 initial powder mixtures

The TiO_2 sintering additive had a positive effect on the densification of hot pressed samples. The positive effect of TiO_2 additive concentration in the initial powder mixture on the densities of hot pressed ceramic composite materials is presented in Fig. 1. The sample with a minimal TiO_2 concentration of 10 wt.% reached the relative density of only 92.1%. Intensive improvement of the density was observed in the interval from 10 to 35 wt.% TiO_2, and from 92.1 to 97.6%. The composites with a sintering additive in the interval from 40 to 50 wt.% TiO_2 reached densities from 99.3 to 99.6%. The samples with 45 wt.% TiO_2 additive concentration reached the highest average density of 99.6%, but samples from 40 to 50 wt.% TiO_2 overlapped partially, and had an average density of 99.5% which was measured with samples with 50 wt.% TiO_2. An increase of hot-pressing temperature would be necessary to densify samples with a concentration of TiO_2 additives below 35 wt.%, but it led to grain coarsening.

Relative high weight loss was measured after hot pressing of composites and this was caused by creating a high portion of volatile components during hot pressing of B_4C with TiO_2. The portion of volatile

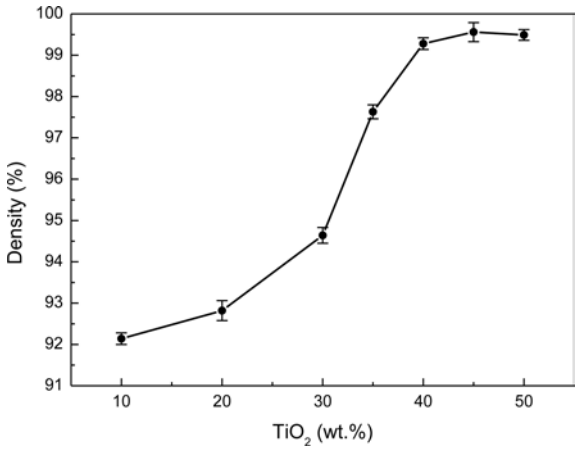

Fig. 1. The effects of TiO_2 sintering additive concentration in the initial powder mixtures on the relative density of B_4C-TiB_2 composites

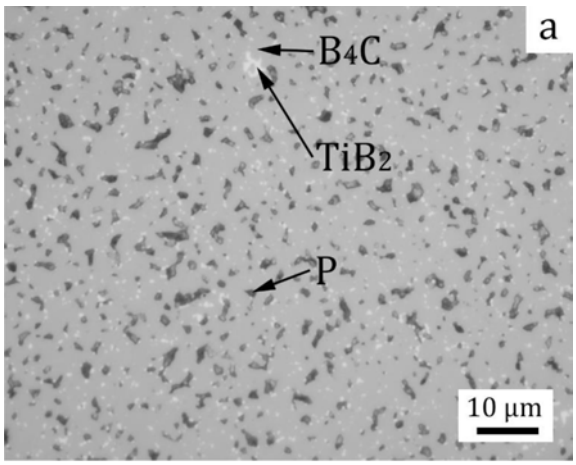

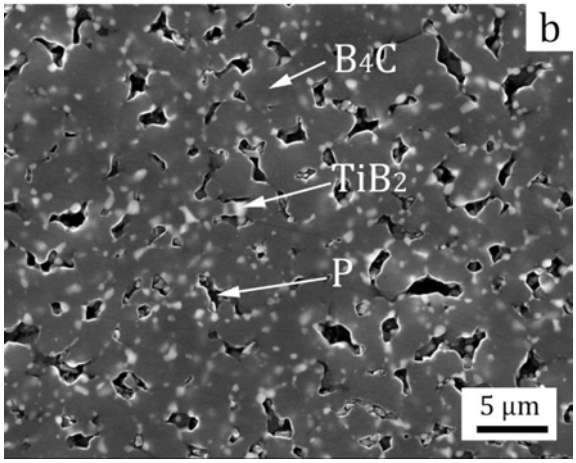

Fig. 2. Microstructure of B_4C-TiB_2 composite with 3.9 vol.% TiB_2, P – porosity a) LM, b) SEM.

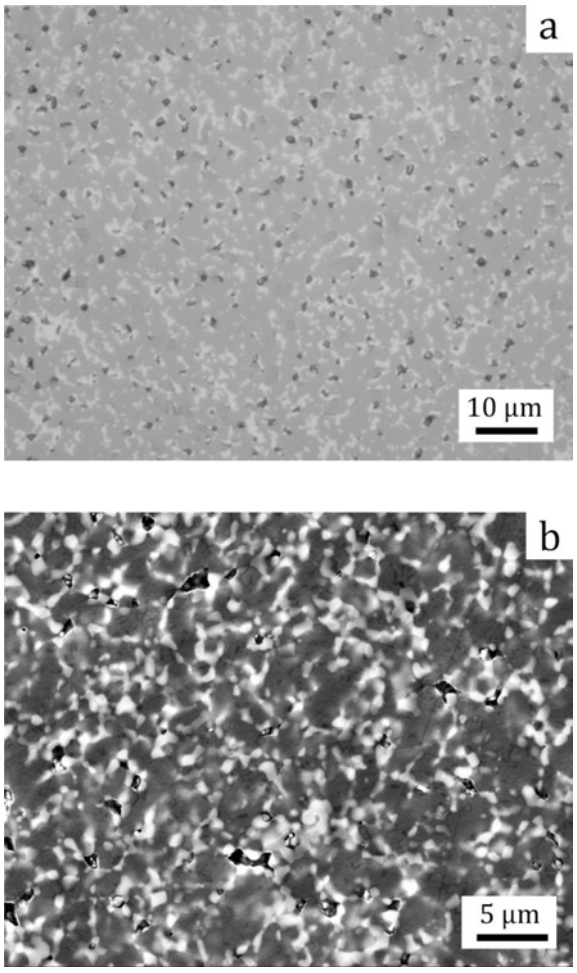

Fig. 3. Microstructure of B_4C-TiB_2 composite with 20.8 vol.% TiB_2, a) LM, b) SEM.

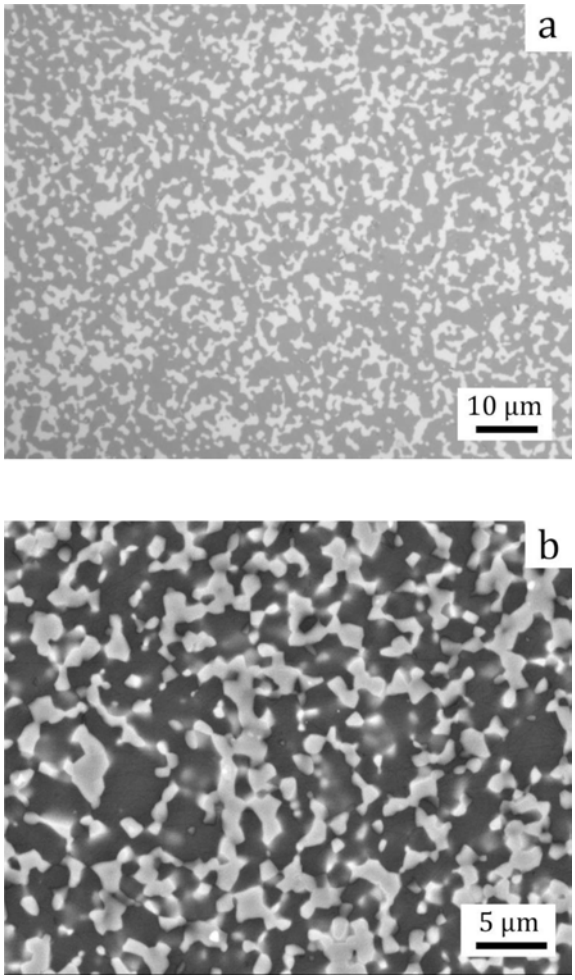

Fig. 4. Microstructure of B_4C-TiB_2 composite with 29.8 vol.% TiB_2, a) LM, b) SEM.

components changed depending on TiO_2 additive concentration in the initial powder mixtures and reached 30 wt.% for samples with the highest TiO_2 concentration in the initial powder mixture.

Microstructure of B_4C-TiB_2 composite

The microstructures of B_4C-TiB_2 ceramic composites with different portion of created phases are documented in two magnifications by light and electron microscopy from Fig. 2 to 6. From these Figures, the effect of the initial composition on both the final phase composition and the densification of composites can be seen. The microstructure of all hot-pressed ceramic composites consisted of the same phases, but with different portions. These phases were identified as a B_4C matrix (grey areas) and TiB_2 secondary phase (light areas) which was created by in-situ sintering reactions. Rest porosity (dark areas) was observed in the samples with lower densities and lower concentration of TiO_2 additive in B_4C and TiO_2 initial powder mixture (see Fig. 2 and 3). The portion of TiB_2 secondary phase increases with concentration of TiO_2 additive in the initial powder mixture consisting of B_4C and TiO_2. TiB_2 secondary phase in Fig. 2 occupies only 3.9 vol.% in the sample prepared by hot pressing of the initial powder mixture with 10 wt.% TiO_2 additive. This sample has the highest portion of porosity about 7.9 vol.% and therefore has the lowest density (see Fig. 1). The portion of the TiB_2 secondary phase in Fig. 3 depicts the microstructure of a sample with a 30 wt.% TiO_2 additive, has a 20.8 vol.% TiB_2 secondary phase and significant reduction of porosity (2.4 vol.%). The microstructure of B_4C-TiB_2 ceramic composites hot pressed with a TiO_2 additive in the interval from 40 to 50 vol.% reached relative density above 99.3% and were without visible porosity as can be seen in Fig. 4, 5 and 6.

The identification of both phases B_4C matrix, and TiB_2 secondary phase was confirmed by X-ray diffraction analysis. X-ray record from analysis of sample with 40 wt.% TiO_2 additive in the initial powder mixture is documented in Fig. 7. The phase analysis of a sample using X-ray diffraction confirmed the creation of composite consisting only of two phases, boron carbide

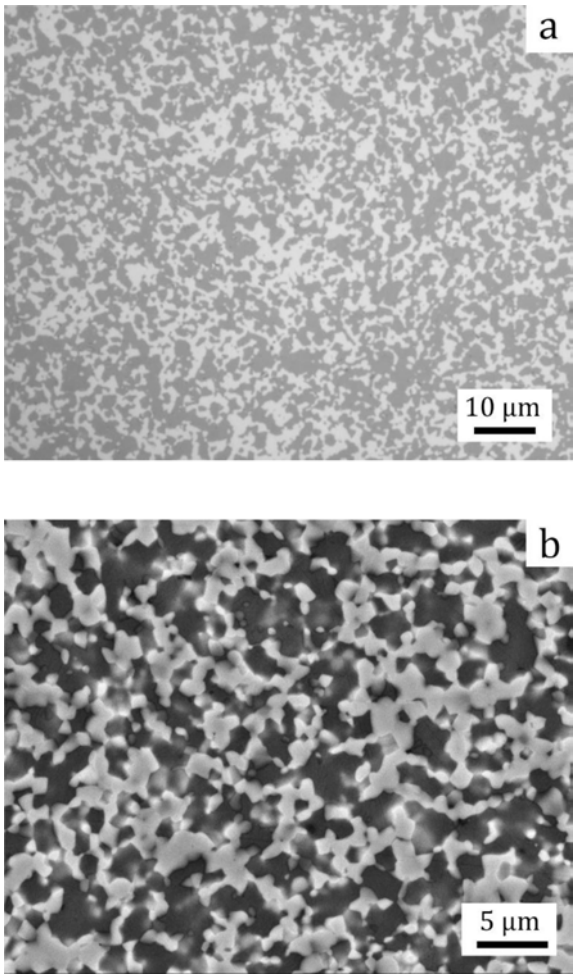

Fig. 5. Microstructure of B_4C-TiB_2 composite with 36.9 vol.% TiB_2, a) LM, b) SEM.

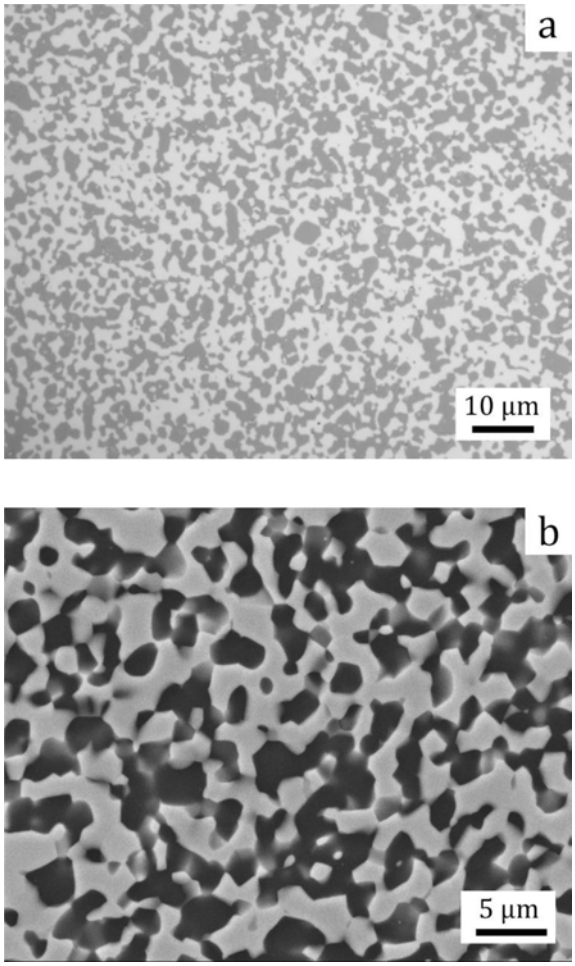

Fig. 6. Microstructure of B_4C-TiB_2 composite with 40.2 vol.% TiB_2, a) LM, b) SEM.

B_4C and titanium diboride TiB_2 with portion of 29.8 vol.% TiB_2 phase. All other samples showed the same two phases but with different intensities from created phases.

The effect of TiO_2 additive concentration on the portion of TiB_2 secondary phase created during the in-situ reaction in B_4C-TiB_2 ceramic composites was measured using image analysis and is documented in Fig. 8. The portion of TiB_2 phase increased almost linearly in B_4C-TiB_2 ceramic composites with the increase of TiO_2 additive concentrations in the initial B_4C and TiO_2 powder mixture in the whole studied concertation range as can be seen in Fig. 8. It increased from an average portion of 3.5 vol.% TiB_2 when adding 10 wt.% TiO_2 to 40.2 vol.% TiB_2 and when adding of 50 wt.% TiO_2 sintering additive into the initial powder mixture.

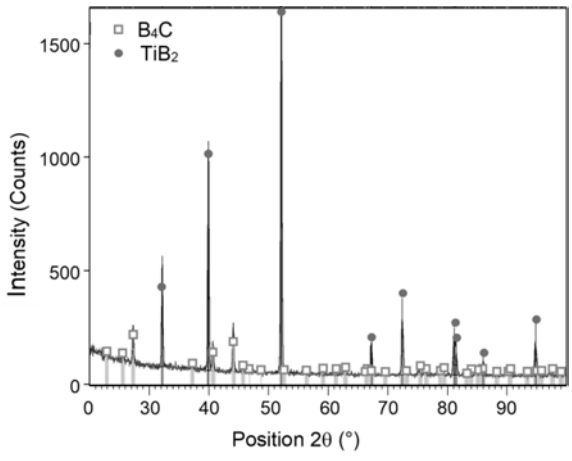

Fig. 7. X-ray record of a sample with 40 wt.% of TiO_2 addition in the initial powder mixture.

Mechanical properties of B_4C-TiB_2 composite

Proper load value which could create cracks in the corners of impression and would not break off the impression was determined at hardness and fracture toughness measurement by a Vickers indenter. The applied load of 5 kP (49.03 N) suited to these requirements as good visible cracks initiated at this load. The effect of TiB_2 portion on the hardness of

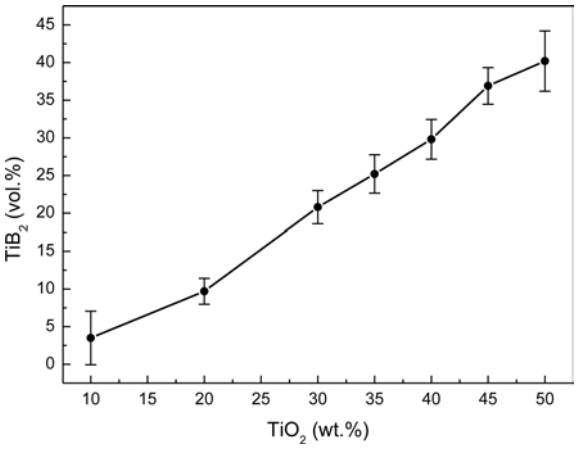

Fig. 8. The effect of TiO_2 sintering additive concentration in the initial powder mixtures on TiB_2 secondary phase portion created in B_4C-TiB_2 composites.

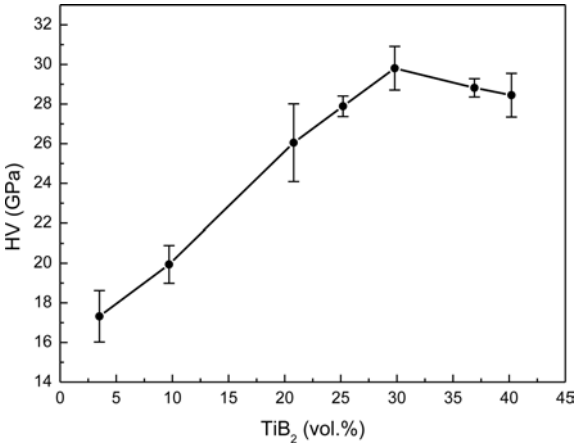

Fig. 9. The effect of TiB_2 portion on the hardness of B_4C-TiB_2 composite.

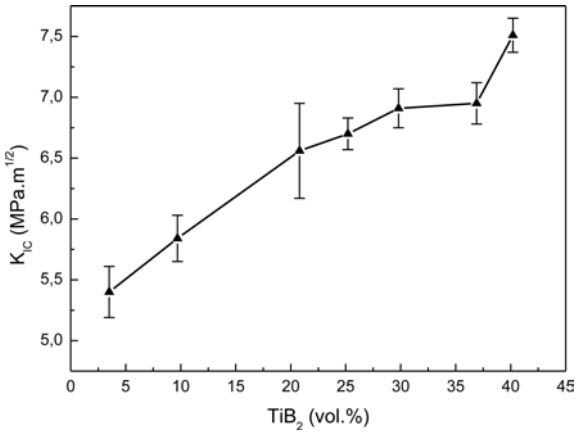

Fig. 10. The effect of TiB_2 portion on the fracture toughness of B_4C-TiB_2 composite.

B_4C-TiB_2 ceramic composite is depicted in Fig. 9. The hardness of B_4C-TiB_2 composite increased to the average value of 29.8 GPa with increased portion of TiB_2 up to the value of 29.7 vol.%. This portion represents the initial concentration of 40 wt.% TiO_2 sintering additive. Thereafter the hardness decreased, and it agrees with the fact that higher portions of TiB_2 phase with lower hardness compared to B_4C phase causes the decrease of the overall hardness of B_4C-TiB_2 composite. Lower hardness values of B_4C-TiB_2 composite at lower portion of TiB_2 phase can be explained by non-sufficient densification of the samples with additive concentration below 35 wt.% TiO_2 in the initial powder mixture. This fact confirms also the effect of the initial powder mixture composition on the density of samples in Fig. 1 and the microstructures of samples in Fig. 2 and 3. The hardness values achieved for B_4C-TiB_2 ceramic composites (Fig. 9) could be compared with results of several works with different portion of TiB_2 secondary phase. In the work [14], the Vickers hardness achieved maximal value of 29.5 and 28 GPa for B_4C-TiB_2 composites with 10 and 30 vol.% TiB_2, respectively. In B_4C-TiB_2 ceramic composites with 25, 30, 43 and 60 vol.% TiB_2 the hardness values of 32.2 GPa [38], 39.3 GPa [39], 25.9 GPa [40], and 29.45 GPa [41], respectively were reported. Reported hardness values are in a good accordance with the values measured in our work.

The effect of TiB_2 portion on the fracture toughness of B_4C-TiB_2 composite is presented in Fig. 10. The fracture toughness increased with the increased portion of TiB_2 in the whole studied range and maximal value of 7.51 $MPa.m^{1/2}$ was achieved for 40.2 vol.% TiB_2 phase, what corresponds to 50 wt.% TiO_2 additive in the initial powder mixture. This fact stems from both better densification of samples with higher concentration of TiO_2 sintering additive, and higher fracture toughness of TiB_2 phase compared to B_4C phase and confirms the toughening effect of TiB_2 phase in B_4C-TiB_2 composite. Measured fracture toughness values could be compared with the results of several works describing B_4C-TiB_2 composites with various portion of TiB_2. In B_4C-TiB_2 composites with 30, 40 43, 60, and 75 vol.% of TiB_2 secondary phase the fracture toughness values of 3.0 [39], 8.2 [14], 8.7 [40], 4.5 [41], and 5.01 $MPa.m^{1/2}$ [38], respectively were reported. These results confirm that our values of fracture toughness are comparable with published results measured for B_4C-TiB_2 composites.

Conclusions

B_4C-TiB_2 ceramic composite materials were hot pressed at a temperature of 1850 °C and a pressure of 35 MPa for 60 min in a vacuum atmosphere from an initial powder mixture consisting of B_4C and TiO_2 additives in concentration intervals from 10 to 50 wt.% TiO_2. TiB_2 secondary phase which was created in the microstructure of the composites utilising in-situ reaction had positive effects on both densification and

mechanical properties of B_4C-TiB_2 composites.

The addition of TiO_2 sintering additive had a positive effect on sample densities. The composites with sintering additives from 40 to 50 wt.% TiO_2 reached relative densities above 99.3%. The samples with concentrations below 35 wt.%, the TiO_2 additive in the initial powder mixture did not reach the required densification and their properties had lower values compared to the samples with higher initial TiO_2 concentration.

The microstructure of all ceramic composites consisted of B_4C matrix, TiB_2 secondary phase created by in-situ sintering, and some rest porosity in the samples with lower densities and lower concentration of TiO_2 additive in the initial powder mixture. The portion of TiB_2 phase increased almost linearly from 3.9 to 40.2 vol.% TiB_2 in B_4C-TiB_2 ceramic composite with the increase of TiO_2 additive concentration from 10 to 50 wt.% TiO_2 in the initial B_4C and TiO_2 powder mixtures.

The hardness of B_4C-TiB_2 composites increased with the increased portion of TiB_2 phase up to the value of 29.7 vol.% TiB_2 and reached the average value of 29.8 GPa. The portion of 29.7 vol.% TiB_2 phase was achieved by reactive hot pressing of the initial powder mixture with 40 wt.% TiO_2 additive.

The fracture toughness increased with the increased portion of TiB_2 phase in the whole experimental concentration range and reached the maximal value of 7.51 MPa.$m^{1/2}$ for 40.2 vol.% TiB_2 phase, which corresponds to 50 wt.% TiO_2 additive in the initial powder mixture.

Acknowledgements

This work was supported by Scientific Grant Agency of the Ministry of Education, Science, Research and Sport of the Slovak Republic under the VEGA 1/0298/18 contract. The work was also supported by UVP STU Bratislava ITMS 26240220084 project.

References

1. B.M. Moshtaghioun, F.L. Cumbrera, A.L. Ortiz, M. Castillo-Rodriguez, and D. Gomez-Garcia, J. Eur. Ceram. Soc. 34[3] (2013) 841-848.
2. R. Lu, S. Chandrasekaran, W.L. Du Frane, R.L. Landingham, M.A. Worsley, and J.D. Kuntz, Mater. Des. 148 (2018) 8-16.
3. X. Li, Y. Gao, L. Song, Q. Yang, S. Wei, L. You, Y. Zhu, G. Zhang, L. Xu, and B. Yang, Ceram. Int. 44[6] (2018) 6443-6450.
4. X. Li, D. Jiang, J. Zhang, Q. Lin, Z. Chen, and Z. Huang, Ceram. Int. 40[3] (2014) 4359-4366.
5. J. Sun, C. Liu, and C. Duan, Mater. Sci. Eng., A 509[1-2] (2009) 89-93.
6. D. Wang, S. Ran, L. Shen, H. Sun, and Q. Huang, J. Eur. Ceram. Soc. 35[3] (2015) 1107-1112.
7. B.M. Moshtaghioun, A.L. Ortiz, D. Gomez-Garcia, and A. Dominguez-Rodriguez, J. Eur. Ceram. Soc. 33[8] (2013) 1395-1401.
8. H. Miyazaki, Y. Zhou, H. Hyuga, Y. Yoshizawa, and T. Kumazawa, J. Eur. Ceram. Soc. 30[4] (2010) 999-1005.
9. S. Hayun, V. Paris, M.P. Dariel, N. Frage, and E. Zaretzky, J. Eur. Ceram. Soc. 29[16] (2009) 3395-3400.
10. C. Wang, Z. Lu, and K. Zhang, Powder Technol. 228 (2012) 334-338.
11. E.W. Neuman, H.J. Brown-Shaklee, G.E. Hilmas, and W.G. Fahrenholtz, J. Am. Ceram. Soc. 101[2] (2018) 497-501.
12. D. Wang, H. Sun, Q. Deng, Z. Ding, S. Ran, and Q. Huang, Ceram. Int. 40[9] (2014) 15341-15344.
13. Q. Wen, Y. Tan, Z. Zhong, H. Zhang, and X. Zhou, Mater. Sci. Eng., A 701 (2017) 338-343.
14. Y. Wang, H. Peng, F. Ye, and Y. Zhou, Transaction of Nonferrous Metal Society of China 21[2] (2011) 369-373.
15. Y. Gao, T. Tang, C. Yi, W. Zhang, D. Li, W. Xie, W. Huang, and N. Ye, Mater. Des. 92 (2016) 814-822.
16. I. Bogomol, P. Badica, Y. Shen, T. Nishimura, P. Loboda, and O. Vasylkiv, J. Alloys Compd. 570 (2013) 94-99.
17. X.Y. Yue, J.J. Wang, X.M. Li, L. You, and H.Q. Ru, Mater. Sci. Eng., A 559 (2013) 719-724.
18. R. Sedlak, A. Kovalcikova, E. Mudra, P. Rutkowski, A. Dubiel, V. Girman, R. Bystricky, and J. Dusza, J. Eur. Ceram. Soc. 37[12] (2017) 3773-3780.
19. C. Xu, Y. Cai, K. Flodstrom, Z. Li, S. Esmaeilzadeh, and G.-J. Zhang, Int. J. Refract. Met. Hard Mater. 30[1] (2012) 139-144.
20. Y. Qiao, L. Qu, X. Zhang, and H. Zhang, Ceram. Int. 41[3] (2015) 5026-5031.
21. X. Zhang, Z. Zhang, R. Wen, G. Wang, X. Zhang, J. Mu, H. Che, and W. Wang, Ceram. Int. 44[2] (2018) 2615-2619.
22. X. Zhang, Z. Zhang, B. Nie, H. Chen, Y. Wang, L. Zheng, Y. Bai, and W. Wang, Ceram. Int. 44[9] (2018) 10766-10772.
23. S. Hayun, S. Kalabukhov, V. Ezersky, M.P. Dariel, and N. Frage, Ceram. Int. 36[2] (2010) 451-457.
24. I. Bogomol, H. Borodianska, T. Zhao, T. Nishimura, Y. Sakka, P. Loboda, and O. Vasylkiv, Scripta Mater. 71 (2014) 17-20.
25. P. Badica, H. Borodianska, S. Xie, T. Zhao, D. Demirskyi, P. Li, A.I.Y. Tok, Y. Sakka, and O. Vasylkiv, Ceram. Int. 40[2] (2014) 3053-3061.
26. X. Zhang, Z. Zhang, W. Wang, J. Shan, H. Che, J. Mu, and G. Wang, J. Am. Ceram. Soc. 100 (2017) 3099-3107.
27. Q.-C. Ma, G.-J. Zhang, Y.-M. Kan, Y.-B. Xia, and P.-L. Wang, Ceram. Int. 36[1] (2010) 167-171.
28. W. Ji, R.I. Todd, W. Wang, H. Wang, J. Zhang, and Z. Fu, J. Eur. Ceram. Soc. 36[10] (2016) 2419-2426.
29. R. Wei, Y. Zhang, H. Gong, Y. Jiang, and Y. Zhang, Ceram. Int. 39[6] (2013) 6449-6452.
30. A. Moradkhani, H. Baharvandi, and M.H.M. Samani, Mater. Sci. Eng., A 665 (2016) 141-153.
31. C. Wu, S. Xie, and Y. Li, Int. J. Appl. Ceram. Technol. 14[6] (2017) 1055-1061.
32. M. Mashhadi, E. Taheri-Nassaj, M. Mashhadi, and V.M. Sglavo, Ceram. Int. 37[8] (2011) 3229-3235.
33. K. Sairam, J.K. Sonber, T.S.R.Ch. Murthy, C. Subramanian, R.C. Hubli, and A.K. Suri, Int. J. Refract. Met. Hard Mater. 35 (2012) 32-40.
34. K. Sairam, B. Vishwanadh, J.K. Sonber, T.S.R.Ch. Murthy, S. Majumdar, T. Mahata, and B. Basu, J. Am. Ceram. Soc. 101[6] (2018) 2516-2526.
35. X. Zhang, H. Gao, Z. Zhang, R. Wen, G. Wang, J. Mu, H. Che, and X. Zhang, Ceram. Int. 43[8] (2017) 6345-6352.

36. H. Latifi, A. Moradkhani, H. Baharvandi, and J. Martikainen, Mater. Des. 62 (2014) 392-400.
37. R.M. White, and E.C. Dickey, J. Eur. Ceram. Soc. 34[9] (2014) 2043-2050.
38. S. Failla, C. Melandri, L. Zoli, G. Zucca, and D. Sciti, J. Eur. Ceram. Soc. 38[9] (2018) 3089-3095.
39. S.G. Huang, K. Vanmeensel, O. Van der Biest, and J. Vleugels, J. Eur. Ceram. Soc. 31[4] (2011) 637-644.
40. X.Y. Yue, S.M. Zhao, L. Yu, and H.Q. Ru, Key Eng. Mater. 434-435 (2010) 50-53.
41. Y.P. Delgado, M.H. Staia, O. Malek, J. Vleugels, and P. De Baets, Wear 317[1-2] (2014) 104-110.